A&A 437, 525–530 (2005)
DOI: 10.1051/0004-6361:20040448

Astronomy & Astrophysics

An emission ring at 20.5 μm around the HAEBE star AB Aurigæ: Unveiling the disk structure

E. Pantin[1], J. Bouwman[1,2], and P. O. Lagage[1]

[1] CEA/Saclay, DSM/DAPNIA/Service d'Astrophysique, 91191 Gif-sur-Yvette, France
e-mail: epantin@cea.fr
[2] Max-Planck-Institut für Astronomie, Königstuhl 17, 69117 Heidelberg, Germany

Received 14 October 2003 / Accepted 25 January 2005

Abstract. Isolated Herbig Ae/Be stars are believed to be a class of objects at an intermediate stage between young stellar objects surrounded by massive, optically thick, gaseous and dusty disks and Vega like stars surrounded by debris disks. The Herbig Ae star AB Aurigæ is already known for being surrounded by an intermediate-stage dust disk emitting a fairly large infrared and (sub-)millimetric excess. Until now, its outer disk structure has only been resolved at millimeter wavelengths and at optical and near infrared wavelengths with coronographic imaging. We have obtained 20.5 μm images which show an unexpected elliptical ring-like emission structure in the disk around AB Aurigæ at a distance of about 280 AU from the central star. This structure is characterized by a large azimuthal asymmetry in its brightness profile and an off-centered position with respect to the central star. To explain the observations, we propose a simple, purely geometrical model based on an emission ring with an uniform surface brightness, but having an intrinsic eccentricity. Our modeling of this ring-like structure provides valuable constraints on the inclination and the dust composition of the disk. Given the large distance from the central star, only transient heating of very small particles can explain the occurrence of the bright emission ring at mid-infrared wavelengths. Our observations point towards an unexpected geometry of the pre-main-sequence disk. In contrast to the usual sketch of a disk having a constant flaring angle, we argue that the circumstellar disk has a sudden, non uniform increase in the disk thickness. This sudden increase in the disk thickness as inferred by our modeling could be caused by disk instabilities. This suggests, together with the derived intrinsic eccentricity of the emission ring, the presence of a still undetected massive planetary type object, in an orbit at the outer-parts of the disk, disturbing the disk structure through gravitational interaction.

Key words. circumstellar matter – stars: formation – stars: pre-main-sequence

1. Introduction

Herbig Ae/Be (HAEBE) stars represent a class of intermediate mass, pre-main-sequence (PMS) stars, first described as a group by Herbig (1960). The circumstellar (CS) disks found around these stars are believed to be the sites of on-going planet formation. By studying the characteristics and evolution of the CS disk and its dust composition, valuable insights can be obtained into the processes leading to the formation of planets, and put constraints on disk and planet formation models. Infrared spectroscopy obtained with the Infrared Space Observatory (ISO) has given us insight into the dust composition of a sample of isolated HAEBE systems (e.g. Bouwman et al. 2000a, 2001; Meeus et al. 2001). While these spectra reveal a rich mineralogy, no direct information concerning the spatial distribution of the different dust species can be inferred from the ISO data. Most studies so far have used the available spectral energy distributions (SEDs) to put constraints on the spatial distribution of the CS material. Models for passively heated disks surrounding PMS stars are successful in reproducing the ISO spectra (e.g. Dullemond et al. 2001; Dominik et al. 2003), but these models cannot be uniquely constrained from SED fitting alone (e.g. Bouwman et al. 2000b). For this, spatially resolved imaging as presented in this paper is required.

Among the isolated HAEBE systems, the disk around AB Aurigæ is one of the most interesting and well studied objects. Its star has a probable age of 2 Myr (van den Ancker et al. 1997), indicating that, according to current planet formation theories, planet building could still being ongoing in this system. ISO spectra show strong emission bands from polycyclic aromatic hydrocarbons (PAH) molecules, and emission from various dust species such as silicates, and carbonaceous dust grains (van den Ancker et al. 2000; Bouwman et al. 2000a). Though the inferred grain sizes are differing from interstellar grains, the dust around AB Aur seems to be relatively unprocessed, indicating an evolutionary young system. This is also suggested by the combined ISO-SWS and submillimeter observations of H_2 and CO rotational lines, which demonstrate that the disk still has a large gas content (Thi et al. 2001). The AB Aurigæ disk has been resolved in the millimeter range by Mannings & Sargent (1997), showing a structure consistent with a Keplerian disk. Its surrounding nebulae and outer disk structure were also studied in the visible range

using broad-band coronographic observations (Grady et al. 1999), showing a disk with spiral-shaped structures. Similar spiral-like structures can also be seen in near-IR coronographic observations obtained with the Subaru telescope (Fukagawa et al. 2004). Near-IR interferometric observations (Millan-Gabet et al. 1999, 2001; Eisner et al. 2003) have resolved the inner parts of the disk. These observations are consistent with the model of a passive disk with an inner hole, seen at a low ($\leq$40°) inclination angle. Recent mid-IR imaging (Chen & Jura 2003), has also resolved the inner disk structure, showing it to originate from thermal emission from dust grains heated by the stellar radiation field near the central star. Here we present mid-IR imaging, not only resolving the thermal emission from dust close to the central star, but also showing an emission structure at the outer parts of the disk. In the next sections we will describe these observations, and propose a simple geometrical model explaining our results.

2. Data collection and reduction

The observations were performed using the CEA mid-IR camera CAMIRAS (Lagage et al. 1992), equipped with a Boeing 128 × 128 pixels BIB detector sensitive up to a wavelength of $\approx$28 μm. AB Aurigæ was observed from the CFH 3.6 m telescope on 1999 August 1 and between 2000 March 16 and March 20. During these two runs, seeing and weather conditions – humidity and amount of atmospheric precipitable water – were particularly favorable and extremely stable in time. We spent a total integration time on AB Aurigæ of 2 h split into several nights. Each dataset was reduced independently in order to avoid any erroneous conclusion due for instance to some corrupted dataset; it permits also to evaluate error bars on our results. The orientation of the array on the sky was carefully determined at the start of each observing run. The pixel size was 0.29″. In the 20 μm window, we used a filter centered at 20.5 μm and with a bandpass (*FWHM*) $\Delta\lambda$ = 1.11 μm. This filter is free of any important atmospheric line contribution. The source was always observed at an airmass of less than 1.3. Standard chopping and nodding techniques were applied with a chopping throw of 16″ North and nodding amplitude of 20″ West. A shift-and-add procedure was applied to each final cube of images using a correlation based method with a re-sampling factor of 4:1. In order to get the best spatial resolution in the dataset, the nodding direction was perpendicular to the chopping direction, resulting in an image containing four times the image of the source. The four sources were extracted and co-added using a cross-correlation method. Finally, each independent dataset was deconvolved separately before co-addition to produce the final image. The peak signal-to-noise ratio in the various datasets ranges from 225 to 255. The standard star α Tau was frequently monitored for further data photometric calibration and for PSF measurements. Because final co-added images are strongly limited in spatial resolution by the seeing and above all by the 3.6 m telescope diffraction-pattern (*FWHM* of 1.4″ at 20.5 μm), the use of deconvolution techniques is mandatory in order to recover the best spatial resolution in mid-IR images. We used the Multiscale Maximum Entropy Method developed by Pantin & Starck (1996) based upon wavelet analysis based on the concept of multiscale information. Shannon theorem prescription allows to pursue the deconvolution down to twice the pixel size, in this case down to $\approx$0.6″, and iterations are stopped according to the residual map (i.e. the data minus the re-convolved solution), which properties should be consistent with noise characteristics. Each epoch dataset was processed (including image deconvolution) independently in order to check the consistency of the results.

3. Results and discussion

3.1. Emission structures and photometry

After deconvolution, the 20.5 μm image of AB Aurigæ shows two main structures, as can be seen in the left panel of Fig. 1. The most striking one is a narrow ring-like structure slightly open (i.e. the flux is decreased by an order of magnitude) in the SW direction. It has a total flux of 2.7 ± 0.3 Jy (taking into account deconvolution errors) and is located at an average distance of 1.94″ (280 AU, assuming a distance of 144 pc) and with a typical width *FWHM* of 0.45″ (65 AU). The ring structure isophotes can be fitted by an ellipse with an eccentricity of 0.3 and position angle (with respect to the west direction) of 85°, offset by 0.2″ along the major axis in southward direction, compared with the central emission. The second structure, and brightest, with a total flux of 48.7 ± 5 Jy, is concentrated in the close vicinity of the star. By comparing AB Aurigæ and PSF profiles we find that the central emission is also resolved with a *FWHM* (diameter) of 3 pixels or 0.9″ (130 AU), probably due to thermally emitting dust grains in the inner regions of the circumstellar disk (note that the star emission ($\approx$4 mJy) is negligible at that wavelength).

3.2. Interpretation: Disk structure and the nature of the emitting grain population

Our images show in the inner parts of the disk a similar structure as reported by Chen & Jura (2003), which can be explained by thermal emission from either a disk and/or an envelope. In our schematic view of the disk thermal emission, the resolved inner structure corresponds to thermal emission of hot dust grains between about 10 AU to 65 AU from the star. At these distances the temperature of the dust grains is such that they emit efficiently thermal radiation at wavelengths around 20 μm. Table 1 list the emission properties of this central emission, assuming that it can be represented by a uniform brightness disk. We stress that our approach is only an approximation, and that we will discuss and model this emission from the inner regions extensively in a forthcoming paper.

Here we will concentrate on the intriguing ring-like structure at about 280 AU from the star. The first thing one can note is that thermal emission from grains in radiative equilibrium with he stellar radiation field can be discarded at such a large distance from the star. In these outer regions of the disk, the stellar radiation field will heat dust grains to temperatures of around a 100 K or less. Reproducing the observed flux from the emission ring with grains at these low temperature, would

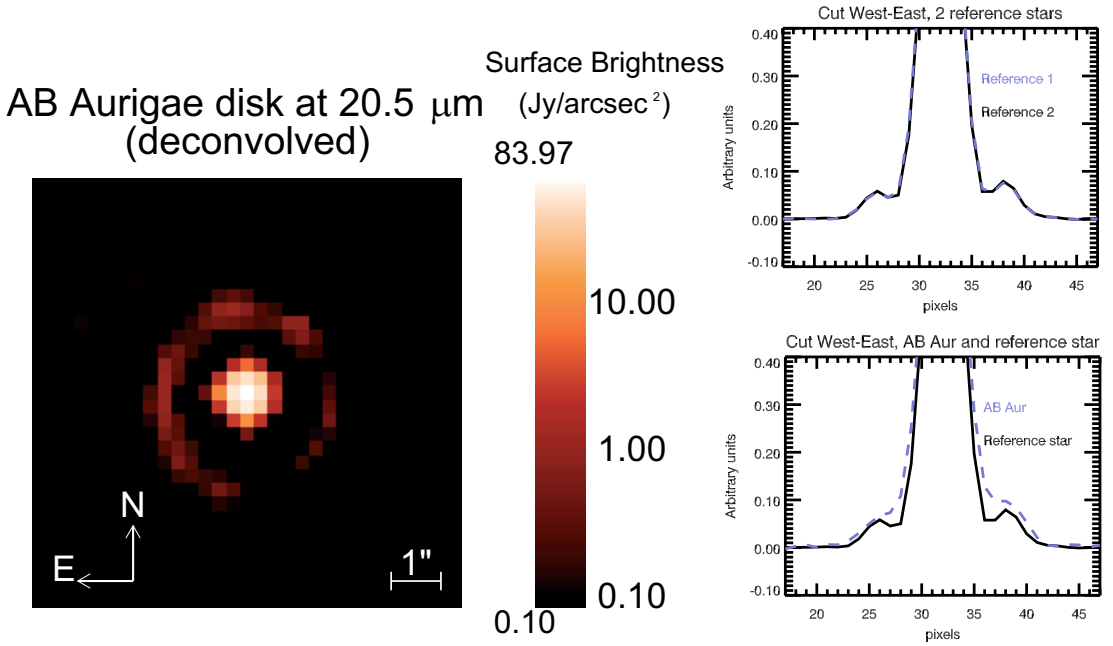

Fig. 1. Image of the AB Aurigae disk at 20.5 μm. The left figure shows the deconvolved image, with a pixel scale of 0.3″/pixel. Clearly visible is a resolved central emission region surrounded by a ring like structure. The panels on the right show the normalized intensity profiles along a cut through the CAMIRAS images of 2 reference stars and AB Aur. The upper right panel shows the comparison between two observations of reference stars, demonstrating the stability of the PSF. The panel on the lower right shows a comparison of AB Aur with the PSF, clearly showing that the central emission is extended and that a ring-like emission structure is also detected in non deconvolved data.

produce such a large flux at wavelengths in the range from 30 to 60 μm that it would be inconsistent with the spectrum as measured by ISO-SWS. Therefore, we must infer stochastically heated very small grains or big molecules like PAHs as the source of the ring-like emission. PAH molecules can be exited at large distances from the central star depending on the the stellar UV field. PAH bands were already found in the ISO-SWS spectrum of AB Aurigæ (van den Ancker et al. 2000; Bouwman et al. 2000a). According to Schutte et al. (1993) and Draine & Li (2001), large PAH molecules (or very small grains), consisting of a few thousand carbon atoms, can efficiently emit infrared radiation with a "plateau"-like spectral shape at around 20 μm. This would be a natural explanation for the observed narrow-band emission of ≈3 Jy at 280 AU from the star. Also, the relative band strength between the emission seen in our images and the PAH bands at shorter wavelengths as observed in the ISO-SWS spectra, is also consistent with the PAH emission models cited above.

The fact that the emission is arranged in a ring puts strong constraints on the disk geometry. In the following we call apparent or projected ellipse the ellipse directly seen on the 20.5 μm image. The most constraining feature of this ring-like elliptical structure is that it is *off-centered along the major axis of the projected ellipse*. In principle, inclining a circular structure leads to a projected elliptical structure that can be off-centered but always *along the apparent minor axis*. Also the systematic brightness variation along the ring is not symmetric with respect to the minor axis of the apparent ellipse (see also the left bottom panel in Fig. 2). This means that either this brightness variation is intrinsic to the ring or that the orientation of the inclination axis is not the same as the major axis of the apparent ellipse. This leads unavoidable to the conclusion that we are looking at an intrinsically elliptical structure seen under a small inclination angle.

Table 1. Best fit model parameters of AB Aur. Listed are the model parameters defining the system orientation, the ring emission and central emission region.

Parameter	Value	±	1σ error
System orientation†:			
Θ	65.699°	±	1.565°
i	−20.904°	±	1.002°
Ring parameters:			
e	0.135	±	0.0063
a	1.955″	±	0.0079″
Φ	123.46°	±	2.65°
ΔR	0.122″	±	0.0086″
H_0	0.469″	±	0.0563″
ΔH	0.177″	±	0.0158″
$I_{\rm ring}$	2.371 Jy arcsec^{-2}	±	0.116 Jy arcsec^{-2}
Parameters central emission:			
$R_{\rm center}$	0.427″	±	0.00122″
$I_{\rm center}$	89.035 Jy arcsec^{-2}	±	0.409 Jy arcsec^{-2}

† Angles are given in degrees counter clockwise with respect to the west direction (right direction).

To determine the main characteristics of the ring structure as seen in the CAMIRAS image of AB Aurigæ, we constructed a simple, geometrical model based on the deconvolved image. Since the inferred very small grains need stellar UV or visible

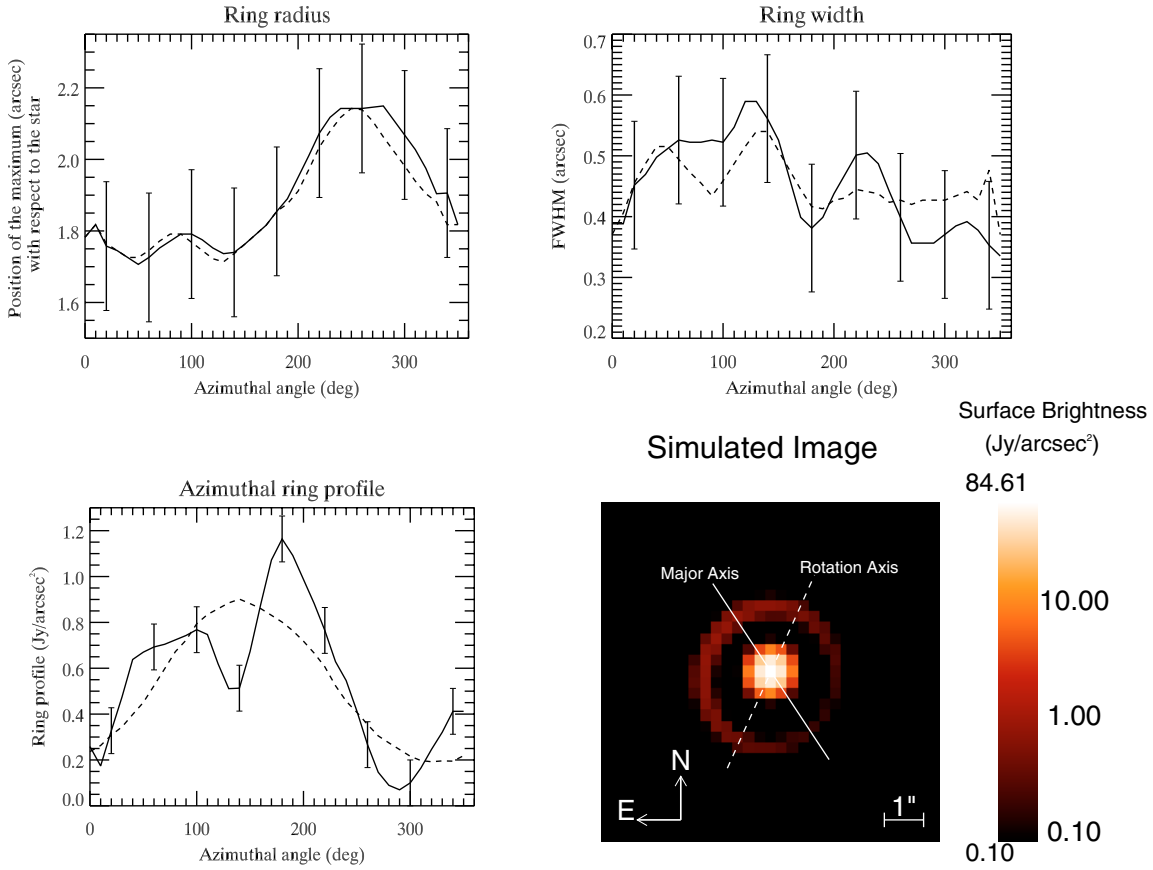

Fig. 2. The structure of the emission ring as an function of azimuth, compared with our best-fit model. Plotted are, *from left to right, top to bottom*, with the solid lines, the ring radius, its width (*fwhm*), and its intensity profile as a function of azimuthal angle (from the west direction, going counter clock wise). Over-plotted with dashed lines are the modeled ring radius, width and intensity profile. For the three solid line plots (data), the profiles have been smoothed by a 5 points (number of angle points being 36) boxcar in order to smooth high frequencies variations. The error bars indicate the formal 1σ error. Also shown is the best fit model image (*bottom right*) with overlaid the rotation axis (link to the disc inclination) and the major axis of the intrinsic ellipse described in Sect. 3.

photons to be excited, their emission most likely originates from the disk surface layer, i.e. the disk photosphere, being directly illuminated by the central star. To mimic this emission from the disk surface layer, we used a uniform brightness ring, with an eccentricity e, semi major axis a, and orientation Φ, radial width ΔR, scale-height H_0, vertical width ΔH, and surface brightness $I_{\rm ring}$. The ring model is positioned such that the central emission is in the focus of the ellipse. The central emission is modeled with a uniform brightness disk with radius $R_{\rm center}$ and surface brightness $I_{\rm center}$. Further, the disk model has a overall inclination i and orientation Θ. The thus constructed projection from this "infinite resolution" model is then convolved with a $\sigma = 0.15$ Gaussian filter to take into account the limited resolution of the deconvolved image ($0.6''$). Our best-fit model (using the 2D fitting procedure MPFIT2DFUN of IDL package written by Markwardt 2002) is shown in Fig. 2 and the resulting fit parameters are listed in Table 1. The parameter values and 1σ errors have been obtained using a so called "boot-strap" method. From the image shown in Fig. 1 we generated 100 additional images by adding Gaussian noise with a distribution corresponding to $1\sigma = 0.1$ Jy/arcsec^2 at each pixel. By performing the identical fitting procedure, resulting each time in slightly different model parameters, a distribution of fitted values for each of the model parameters is thus obtained. The resulting mean and standard deviation of these distributions are quoted in Table 1. We checked that the overall inverse modeling is correct by verifying that our solution also corresponds to a minimum of χ^2 in raw data (non deconvolved) space. Examples of the remaining residuals after subtracting model images from the raw data can be seen in Fig. 3. This excellent agreement between our model with both the deconvolved images as well as the raw data, shows the strength of modern deconvolution techniques. We would like to stress that in many cases model parameters can be degenerated, and many solutions are, therefore, possible. The only solution is to start with a model close to the real solution to avoid falling in a local minimum. In the case of AB Aurigæ this means that without image deconvolution, it would have been impossible to guess that are dealing with a narrow ring at $1.94''$ from the star. The large intrinsic width of the PSF would have prevented this when using solely non-deconvolved images.

A sketch of the derived disk structure is shown in Fig. 4. The appearance of an emission ring can be linked to the disk geometry as follows: in a flaring disk model the amount of radiation intercepted, and thus emitted, is proportional to the angle at which the stellar light impinges onto the disk surface. This

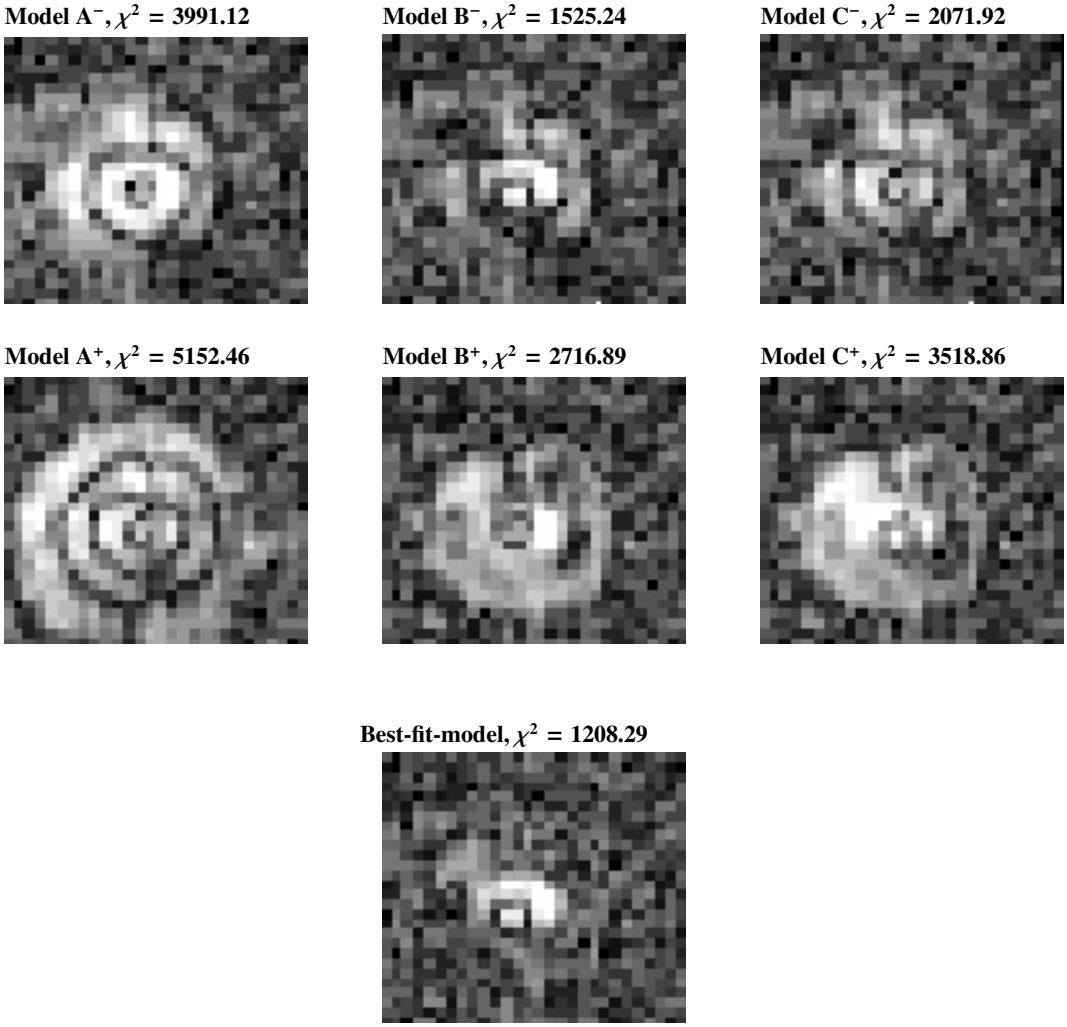

Fig. 3. Residual images of the (non deconvolved) AB Aurigæ observation minus model images. Shown are the residuals for three models (A, B, C), having identical model parameters as listed in Table 1 but with one parameter varied by 20%. The varied parameters for the three models are, respectively, the major axis a, the ring width ΔR and the ring intensity $I_{\rm ring}$. *The top panels* show the models with a minus 20% variation, the lower with a plus 20% variation. Also indicated above each figure is the resulting chi-square value. *The bottom panel* shows the residual for the best-fit model. One can notice that the residuals of the best-fit model still show some structures in the central regions of the disk. This means that our simple model (uniform disk) is not describing perfectly this region; more complex structures with possible offsets from the star will be investigated in a forthcoming paper.

angle is a factor of 15 (with the parameters found in the case of AB Aurigæ) larger at the ring surface compared to a uniform flaring (wedge) disk. This implies that a factor of 15 more light is intercepted and consequently emitted at the disk surface, lifting it above the detection limit of the CAMIRAS instrument. This large flaring angle of the disk surface can also explain the gap in the SW direction, as the disk surface becomes self shadowed when seen under a small inclination of $-20°$. This kind of "puffed-up" structure might be the result of gravitational disk instabilities like those suggested by Boss (2001, 2004) or the result of shadowing instabilities as reported by Dominik et al. (2003). Other possibilities to explain a sudden increase in brightness at a distance of 280 AU, could be:

- dust sizes segregation (Takeuchi & Lin 2003) but one must infer a very peculiar structure of the gaseous disk to reproduce the observations;
- PAH photo-dissociation, but it is unlikely to occur to the inferred population of large PAH molecules (e.g. Allain et al. 1996);
- an hollow spherical shell and its limb brightening, but it is difficult to explain the off-centering with this model.

Any proposed model must be able to explain the origin of the intrinsic eccentricity and off-centering of the emission ring A natural explanation for this could be the presence of a massive perturber on an eccentric orbit. Such an object might produce the detected deformations of the disk trough gravitational interaction. This could also be the explanation for the spiral-like structures seen in optical and near-IR coronographic imaging (Grady et al. 1999; Fukagawa et al. 2004). Given the large distance from the central star at which the emission ring occurs, it is unlikely for the perturbing companion to be a giant planet.

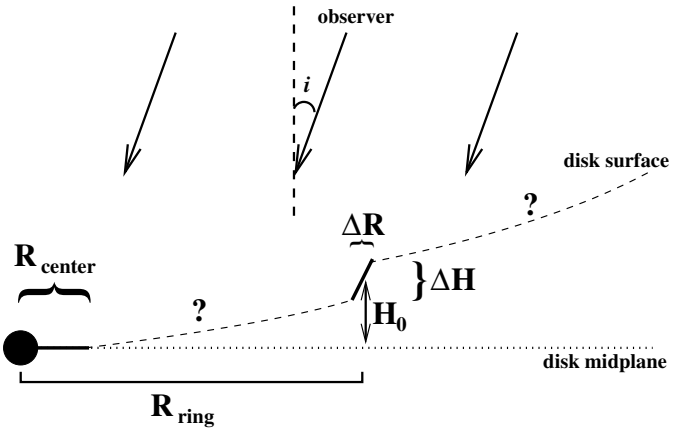

Fig. 4. Schematic representation of the disk structure in the AB Aur system. Drawn is the derived geometry of the disk surface. Indicated in the figure are the model parameters defining this geometry as listed in Table 1. $R_{\rm ring}$ is the distance to the star and varies between $a(1-e)$ and $a(1+e)$.

If the companion hypothesis is correct, it will most likely be a not yet detected brown dwarf.

4. Conclusions

We have presented in this paper a thermal infrared image at 20.5 μm of the AB Aurigæ dusty disk. The deconvolved image shows an inner resolved structure containing the majority (95%) of the thermal flux at this wavelength, together with an unexpected ellipsoidal, ring-like structure at an average distance of 280 AU from the central star. This large distance implies that this emission originates from stochastically heated, PAH like grains. The most interesting features of the ring are the large scale azimuthal asymmetry in its intensity profile and its off-centered position with respect to the position of the central star. When modeling the ring structure using a purely geometrical model (in which asymmetries are essentially produced by inclination and self shadowing effects in a flared disk), we have to conclude that we are observing an *intrinsically ellipse-shaped* ring. The appearance of the ring can be explained by a sudden increase in the scale height of the disk photosphere in an otherwise uniform flaring disk, leading to a kind of "wall-like" structure. This sudden increase of the flaring angle causes the disk to intercept more stellar light and consequently to emit more IR radiation, lifting the emission from the disk surface at the position of the ring above the detection limit of our observations. Disk instabilities perturbing the disk vertical thickness might produce such a structure. However, the origin of its intrinsic eccentricity and off-centered position remains unclear. A natural explanation could be the presence of a massive planetary object or brown dwarf on an elliptical orbit structuring the disk trough gravitational interaction. More detailed modeling and further observations, including higher resolution imaging in several PAH bands and spatially resolved mid-IR spectroscopy, are needed to fully understand the physics of this intriguing structure.

Acknowledgements. We are gratefully indebted to P. Masse, R. Jouan and M. Lortholary for their efficient assistance with the CAMIRAS instrument, A. Claret in efficiently supporting us in our observations, as well as to the staff of CFHT/Hawaii for their support during the observing runs. JB acknowledges financial support by the EC-RTN on "The Formation and Evolution of Young Stellar Clusters" (RTN-1999-00436, HPRN-CT-2000-00155) The observations preparation was done using the SIMBAD database.

References

Allain, T., Leach, S., & Sedlmayr, E. 1996, A&A, 305, 602
Boss, A. P. 2001, ApJ, 563, 367
Boss, A. P. 2004, ApJ, 610, 456
Bouwman, J., de Koter, A., van den Ancker, M., & Waters, L. 2000a, A&A, 360, 213
Bouwman, J., de Koter, A., van den Ancker, M., & Waters, L. 2000b, in Thermal Emission Spectroscopy and Analysis of Dust, Disks, and Regoliths, ASP Conf. Ser., 196, 63
Bouwman, J., Meeus, G., de Koter, A., et al. 2001, A&A, 375, 950
Chen, C. H., & Jura, M. 2003, ApJ, 591, 267
Dominik, C., Dullemond, C. P., Waters, L. B. F. M., & Walch, S. 2003, A&A, 398, 607
Draine, B. T., & Li, A. 2001, ApJ, 551, 807
Dullemond, C. P., Dominik, C., & Natta, A. 2001, ApJ, 560, 957
Eisner, J. A., lane, B. F., Akeson, R. L., Hillenbrand, L. A., & Sargent, A. I. 2003, ApJ, 588, 360
Fukagawa, M., Hayashi, M., Tamura, M., et al. 2004, ApJ, 605, L53
Grady, C. A., Woodgate, B., Bruhweiler, F. C., et al. 1999, ApJ, 523, L151
Herbig, G. H. 1960, ApJS, 4, 337
Lagage, P. O., Jouan, R., Masse, P., Mestreau, P., & Tarrius, A. 1992, in Progress in Telescope and Instrumentation Technologies, 601
Mannings, V., & Sargent, A. I. 1997, ApJ, 490, 792
Markwardt, C. 2002, Markwardt IDl programs, `http://cow.physics.wisc.edu/~craigm`
Meeus, G., Waters, L., Bouwman, J., et al. 2001, A&A, 365, 476
Millan-Gabet, R., Schloerb, F. P., Traub, W. A., et al. 1999, ApJ, 513, L131
Millan-Gabet, R., Schloerb, F. P., & Traub, W. A. 2001, ApJ, 546, 358
Pantin, E., & Starck, J.-L. 1996, A&AS, 118, 575
Schutte, W. A., Tielens, A. G. G. M., & Allamandola, L. J. 1993, ApJ, 415, 397
Takeuchi, T., & Lin, D. N. C. 2003, ArXiv Astrophysics e-prints
Thi, W. F., van Dishoeck, E. F., Blake, G. A., et al. 2001, ApJ, 561, 1074
van den Ancker, M., Bouwman, J., Wesselius, P., et al. 2000, A&A, 357, 325
van den Ancker, M. E., The, P. S., Tjin A Djie, H. R. E., et al. 1997, A&A, 324, L33